Article

Light-Controlled Cell−Cell Assembly Using Photocaged Oligonucleotides

Katelyn Mathis,[§] Afia Ibnat Kohon,[§] Stephen Black, and Brian Meckes*

Cite This: *ACS Mater. Au* 2023, 3, 386−393

Read Online

ACCESS | Metrics & More | Article Recommendations | Supporting Information

ABSTRACT: The interactions between heterogeneous cell populations play important roles in dictating various cell behaviors. Cell−cell contact mediates communication through the exchange of signaling molecules, electrical coupling, and direct membrane-linked ligand−receptor interactions. In vitro culturing of multiple cell types with control over their specific arrangement is difficult, especially in three-dimensional (3D) systems. While techniques that allow one to control the arrangement of cells and direct contact between different cell types have been developed that expand upon simple co-culture methods, specific control over heterojunctions that form between cells is not easily accomplished with current methods, such as 3D cell-printing. In this article, DNA-mediated cell interactions are combined with cell-compatible photolithographic approaches to control cell assembly. Specifically, cells are coated with oligonucleotides containing DNA nucleobases that are protected with photocleavable moieties; this coating facilitated light-controlled cell assembly when these cells were mixed with cells coated with complementary oligonucleotides. By combining this technology with digital micromirror devices mounted on a microscope, selective activation of specific cell populations for interactions with other cells was achieved. Importantly, this technique is rapid and uses non-UV light sources. Taken together, this technique opens new pathways for on-demand programming of complex cell structures.

KEYWORDS: cell−cell contact, heterojunctions, cell communication, co-culturing, 3D cell-printing, DNA programmability, photolithography
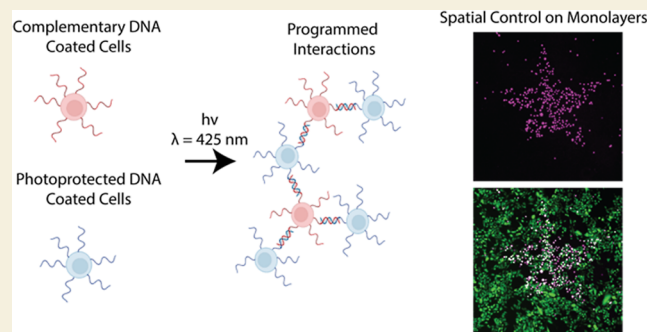
Interactions between heterogeneous cell populations play important roles in dictating diverse cell behaviors that include proliferation,[1] differentiation,[2] and apoptosis.[3] In particular, cell−cell contact mediates communication through the exchange of signaling molecules,[4] electrical coupling,[5] and direct membrane-linked ligand−receptor interactions.[6,7] The arrangement of complex cell mixtures within a tissue results in the formation of cell junctions between different cell types (heterojunctions). These heterojunctions affect the cell behavior by changing gene expression levels,[8,9] inducing cell migration[10−12] and mitochondrial transfer.[13,14] Cell−cell contact between different cell types can lead to the exchange of molecules that are not produced by the original cell type, contributing to dysfunctional disease states or regulating developmental processes. For example, tumor cells can secrete factors that increase endothelial cell proliferation and change the tumor microenvironment.[9] Co-culturing cells of different cell types has proven to be powerful in understanding how cells behave in complex microenvironments.[15−17] A greater understanding of cellular contact-mediated communication between cell types would have important implications for many diseases and tissue functions, such as cancer metastasis,[9,18] heart disease,[19,20] vascularization and angiogenesis,[16] bone remodeling,[17] and the epithelial to mesenchymal transition.[21] Cellular

interactions are especially important for tissues containing rare populations of cells that play important roles in tissue function or disease progression but are difficult to study in isolation due to their low numbers. As examples, certain immune cells such as regulatory T cells[22,23] and dendritic cells[24] are present in low numbers in many tissues but play crucial roles in immune regulation and response. Similarly, stem cells and progenitor cells that are responsible for tissue maintenance and regeneration are often present in small numbers in adult tissues.[25,26] However, in vitro culturing of multiple cell types with control over their specific arrangement is difficult, as spatial and three-dimensional (3D) control over specific cells is not easily accomplished. Technologies that facilitate 3D arrangement of cells would allow for replication of cell structures observed in vivo that more closely represent
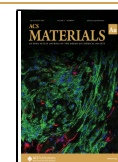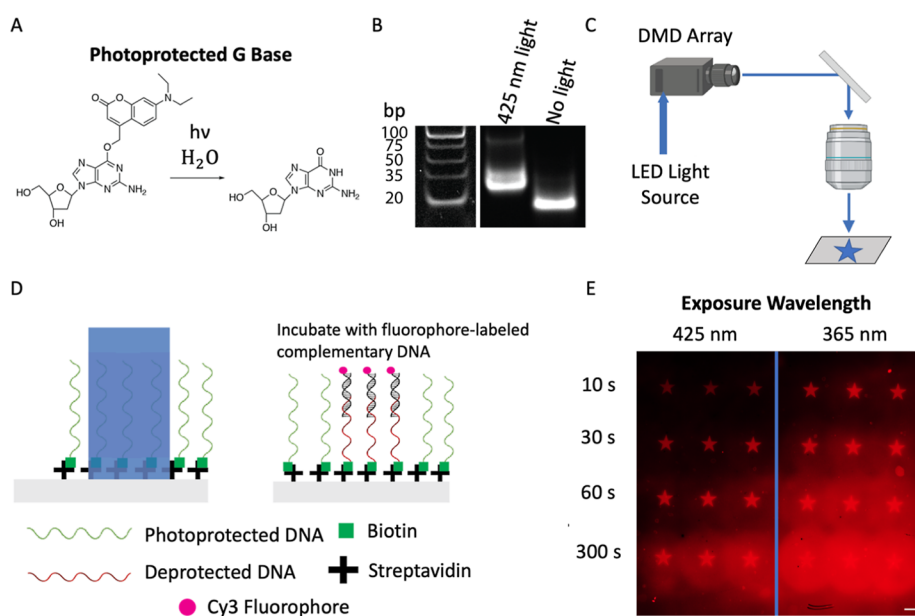
Figure 1. Spatially controlled hybridization on surfaces. (A) Schematic of light-induced removal of a protecting coumarin molecule to create a guanine base. (B) Image of electrophoretic gel of oligonucleotide mixtures consisting of complimentary oligonucleotides with and without light exposure. (C) Schematic of the experimental setup for patterning oligonucleotides. (D) Schematic depicting light-exposed deprotection of biotinylated DNA attached to a streptavidin-coated coverslip. (E) Fluorescent micrograph of photoactivatable DNA-coated surfaces exposed to light at different wavelengths and times and incubated with Cy3-labeled complementary DNA. Scale bar = 500 μm.

physiological behavior, allowing better understanding of rare cell function and potential therapeutic interventions.

Due to the importance of cell−cell contact and cell signaling between different cell types, techniques that allow one to control the arrangement of cells and direct contact between different cell types have been developed that expand upon simple co-culture methods. Devices have been developed for placing two different cell populations in contact with a defined interaction boundary between monolayers.[27,28] More recently, emerging 3D cell-printing has been used to co-culture multiple cell types through the deposition of a "bioink" containing live cells.[11,29,30] Although multiple cell types can be contained within an ink droplet, specific control over the heterojunctions that form between cells is not possible with current 3D cell-printing technologies. Similarly, microfluidic devices allow cells to be systematically added together.[10,14,18] This allows for the creation of heterojunctions, but the control is limited in larger populations along with true 3D placement.

To program specific cell interactions, DNA base pairing has been used to control heterojunction formation. By functionalizing different cells with complementary sequences, control over the cell arrangement has been achieved.[31,32] Additionally, sequence design can be used to control cell assembly rates.[33] Gartner and coworkers have demonstrated the use of oligonucleotide programmability to create a three-dimensional organoid-like tissue embedded in a gel framework.[34] DNA programmability has been extended to place 2D cell populations on surfaces with spatial arrangement.[35−37] More recently, DNA origami structures were used to create multi-cellular interactions with up to three different cell types.[38] These technologies are powerful tools for building complex cell structures; however, they do not allow for on-the-fly patterning in a spatially controlled manner conducive to 3D printing. Methods that combine aspects of stereolithography with DNA programmability to 3D print cells with higher precision in a

spatially encoded fashion would enable the creation of elegant 3D microtissues.

Herein, we combine DNA-mediated cell interactions with cell compatible photolithographic approaches to build de novo cell assemblies in 3D. Specifically, we utilized oligonucleotides containing DNA nucleobases with photocleavable coumarin protecting groups to control cell placement. We show that these oligonucleotides, when attached to glass surfaces or on the surface of cells, can be activated by light, allowing recognition by complementary oligonucleotides in a spatially defined fashion. For cellular programming, cell monolayers coated with photoprotected oligonucleotides were exposed to spatially localized, low toxicity, non-UV light (425−450 nm). Subsequent incubation with cells coated with complimentary oligonucleotides resulted in placement of these cells within the exposed area. Taken together, our studies demonstrate a feasible path to create complex tissue mimics with high reproducibility and control.

■ RESULTS

Light Directed Spatially Controlled Oligonucleotide Binding

In order to dynamically and spatially control the interaction between oligonucleotides, we first synthesized oligonucleotides containing photocleavable protecting groups that have previously been reported for spatio-temporally controlled hybridization.[39−42] These nucleotides consist of guanines modified with coumarin protection groups (5′-dimethoxytrityl-N2-(4-isopropylphenoxyacetyl)-O6-[[7-(diethylamino)-coumarin-4-yl]-methyl]-2′-deoxyGuanosine, 3′-[(2-cyanoethyl)-(N,N-diisopropyl)]-phosphoramidite; DEACM caged dG-CE) where exposure to light from 365 to 505 nm induces the removal of the coumarin group (Figure 1A).[43,44] We chose these structures due to the ability to deprotect the bases with wavelengths that fall outside potentially cytotoxic UV regions.
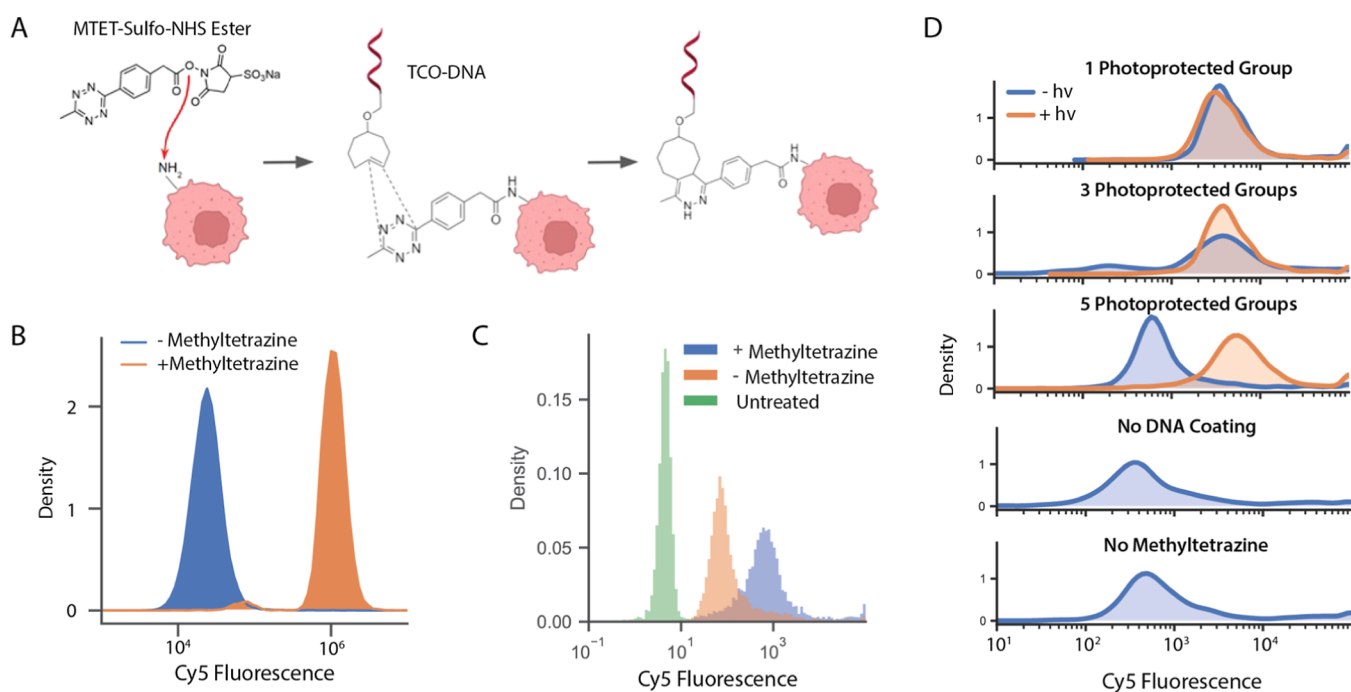
Figure 2. DNA functionalization of cell membranes with photoprotected DNA. (A) Schematic of the two-step functionalization strategy used to attach DNA to the cell surface. (B) Flow cytometry fluorescence intensity measurements of unmodified cells and MTET modified cells upon incubation with Cy5-TCO. (C) Flow cytometry histogram of the Cy5 fluorescence for cells treated with MTET and Cy5-TCO DNA, Cy5-TCO DNA only, and untreated cells. (D) Flow cytometry histograms of the Cy5 fluorescence for cells coated with DNA containing 1, 3, and 5 protecting groups, along with control cells consisting of MTET coating only and unmodified cells upon incubation with Cy5-labeled complementary DNA.

For our initial designs, we included five coumarin photoprotected bases since this has previously been shown to be sufficient to prevent hybridization to complementary strands in RNA interference applications (sequences available in Table S1).[45,46] We chose a conservative number of modifications to ensure that unwanted hybridization could be prevented for patterning. To assess the photocleavability of the oligonucleotides, we incubated photoprotected oligonucleotides (sequence 1, Table S1) with complementary Cy3-labeled DNA (sequence 2, Table S1) in two conditions: (1) with exposure to 450 nm light for 60 s and (2) without any light exposure. Polyacrylamide gel electrophoresis shows that double-stranded structures only formed when oligonucleotides are exposed to light, while unexposed structures showed no meaningful hybridization (Figure 1B). We note that the presence of higher bands in the light exposed lane is the likely result of using repeating sequences (i.e., GGTT and AACC) that would allow for the creating of larger structures due to imperfect hybridization.

Next, we sought to examine spatial control using these oligonucleotides. For these experiments, photoprotected oligonucleotides were synthesized with 3′ biotin (sequence 3, Table S1). These oligonucleotides (containing five photocages) were then incubated with glass substrates that had been coated with streptavidin to facilitate biotinylated oligonucleotide binding (Figure 1D). After incubating with DNA for over 30 min and rinsing with phosphate-buffered saline (PBS), the coverslips were exposed to 365 and 450 nm lights for different periods of time in a recognizable pattern controlled by a digital micromirror device (DMD) (Figure 1C). After light exposure with the DMD array, the surfaces were rinsed with PBS and then incubated with Cy3-labeled complementary DNA (sequence 2, Table S1) for 5 min. The surfaces were then

rinsed three times and imaged under a microscope. Fluorescence micrographs show localized hybridization that reflects the pattern exposed on the surface (Figure 1E). Importantly, our studies show rapid deprotection of the probes at both 365 and 425 nm wavelengths. 365 nm appeared to be more efficient, but not on significantly meaningful periods of time. As exposure times increased, increasing background hybridization due to light scattering was observed, which is indicative of overexposure. These results highlight that we are able to efficiently control hybridization using stereolithographic techniques with biocompatible 425 nm wavelengths. To assess the stability of the patterns, the patterns were incubated in complete growth media at 37 °C. Over time, the pattern fluorescence decreased. However, the patterns are still discernible after 24 h (Figure S1).

Cell Membrane Functionalization with Single-Stranded Oligonucleotides

Our next objective was to implement these oligonucleotides on cell surfaces. To accomplish this goal, we attached the DNA using a two-step process (Figure 2A) to the surface of cells that had been trypsinized and suspended in PBS. First, we incubated cells with a bifunctional linker, methyltetrazine-sulfo-N-hydroxysuccinimide (MTET-NHS ester). The NHS ester reacted with amines on the cell surface resulting in cells with MTET on the surface. MTET modification was used due to its reactive orthogonality to conventional biological groups and its fast kinetics in biological media with transcyclooctene (TCO).[47] Excess unreacted methyltetrazine was removed from the solution by rinsing the cells. To confirm the presence MTET on the cell surface, modified and unmodified cells were incubated with cyanine-5(Cy5)-TCO. Flow cytometry and fluorescence microscopy show elevated fluorescence of cells that had been modified with MTET in comparison to
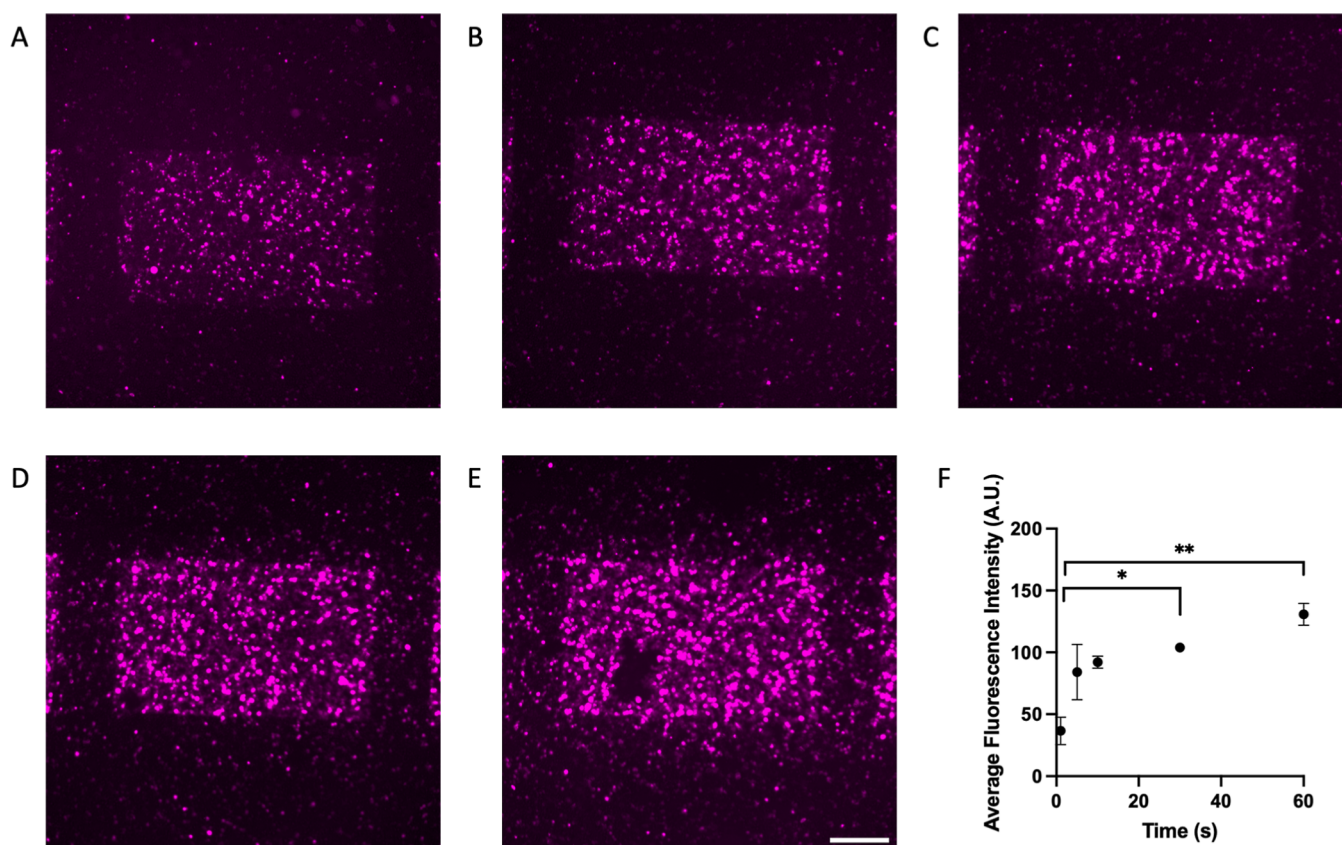
Figure 3. Patterning DNA on cell monolayers. Fluorescence micrographs of cell monolayers coated with photocaged oligonucleotides exposed to 425 nm light for (A) 1 s, (B) 5 s, (C) 10 s, (D) 30 s, and (E) 60 s and then incubated with complementary Cy5-labeled DNA. Scale bar = 500 μm; applies to all images. (F) Average Cy5 intensity within exposed areas for each time point. Error bars denote standard deviation. $*p < 0.05$, $**p < 0.01$; ANOVA with Tukey HSD post hoc analysis.

unmodified cells (Figures 2B and S2), indicating that we had successfully modified the cells.

Next, we incubated MTET modified cells with TCO-terminated DNA for 5 min. To assess attachment to the cell surface, we used Cy5-labeled DNA (sequence 4, Table S1). Excess DNA was removed by pelleting cells and rinsing. Flow cytometry analysis revealed that cells treated with both MTET and TCO-Cy5 DNA exhibited higher fluorescence intensity compared to cells treated with only TCO-Cy5 DNA or the untreated group (Figure 2C). The cells treated with only TCO-Cy5 DNA showed higher fluorescence intensity compared to the untreated group because of uptake of the DNA into the cells, presumably due to the hydrophobicity of the Cy5 group coupled with the use of phosphorothioate DNA. Importantly, we found that our attachment scheme worked across multiple different cell types. NM2C5, M4A4, and 3T3 cells all showed similar amounts of TCO-Cy5-DNA and TCO-Cy5 attachment, indicating that MTET attachment levels were not limiting the attachment of DNA (Figure S3).

To confirm that the photoactivation of oligonucleotides still worked on the cell surface, we incubated MTET modified cells with photoprotected DNA containing a phosphodiester (PO) backbone with 1, 3, or 5 protecting groups (sequences 5−7, Table S1). We exposed the cells to 425 nm light for 1 min, followed by incubation with Cy5-labeled complementary DNA (sequence 8, Table S1). Flow cytometry showed no significant difference in fluorescence of the cells with oligonucleotides with 1 or 3 protecting groups upon exposure to light. However, those with five protecting groups showed increased fluo-

rescence upon light exposure, indicating that five protecting groups are sufficient to fully block interactions with complementary DNA (Figure 2D). The unexposed cells showed fluorescence similar to cells not coated or MTET when treated with Cy5-labeled DNA. Based on these results, we set out to examine if the backbone composition of the oligonucleotide altered interactions on the cell surface. We synthesized phosphorothioate (PS) DNA containing five photocleavable groups (sequence 9, Table S1) and exposed them to light. Coating the cells with phosphorothioate DNA showed increased fluorescence upon light exposure and greater overall fluorescence than PO DNA. However, the non-light exposed cells showed higher fluorescence than the control groups (Figure S4), indicating that the protecting groups were not fully blocking interactions with complementary DNA, while being at higher concentrations on the cell surface.

Next, we sought to evaluate the patterning capabilities of the oligonucleotides on cell monolayers. NM2C5 cells were cultured on plastic Petri dishes until they reached high confluency, and then, coated them with photoprotected DNA (sequence 7, Table S1). The cells were subsequently exposed to 425 nm light in a spatially controlled manner using a DMD mounted on a microscope for different durations (1, 5, 10, 30, and 60 s). After exposure, the cell monolayer was incubated with complementary Cy5-labeled DNA (sequence 8, Table S1) for 5 min. Fluorescence micrographs revealed that the DNA was localized to the areas that were exposed to light, with spatial control achieved with exposure time scales as short as 1 s (Figure 3). Increasing the exposure time resulted in increased
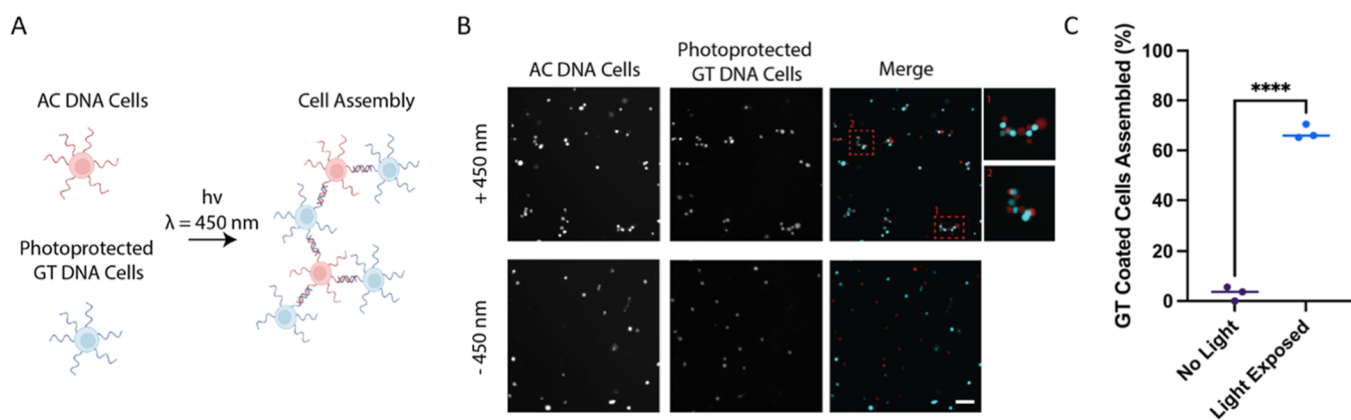
Figure 4. Controlling cell assemblies with light. (A) Schematic of cell assembly upon irradiation with light. (B) Fluorescence micrographs of CTO (AC DNA-coated cells) and CTG (photoprotected GT DNA-coated cells) labeled cells exposed to 450 nm light or unexposed. Scale bar = 200 μm. (C) Percentage of GT DNA cells in assembly for unexposed and light exposed GT DNA coated cells. ****$p < 0.0001$; T-test. Panel A was generated using BioRender.
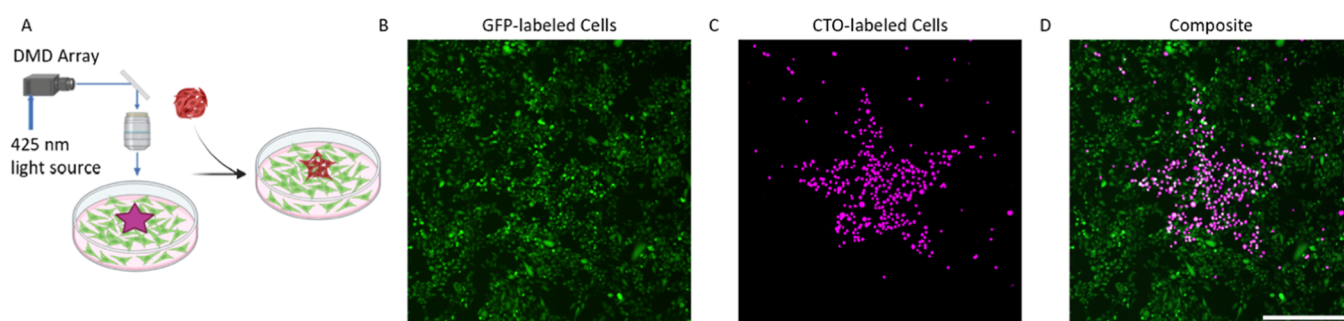
Figure 5. Controlling cell placement on monolayers. (A) Schematic of patterning on the cell monolayer to control cell attachment to irradiated locations. (B−D) Fluorescence micrographs of monolayers of GFP-labeled cells coated with photoprotected DNA upon exposure to 425 nm light and incubation with CTO-labelled cells coated with complementary DNA. (B) GFP channel. (C) TXRED channel. (D) Composite of both channels. Scale bar = 500 μm. Panel A was generated using BioRender.

brightness up to an incubation time of 30 s. However, increasing the exposure duration beyond this time did not result in appreciable increases in fluorescence. These studies highlight the speed of our patterning approach when activating cell surfaces.

Programming Cell−Cell Interactions with Light

To assess whether we could control cellular interactions with light, we fluorescently labeled cells with fluorescently distinct dyes [cell tracker green (CTG) or orange (CTO)]. The CTG-labeled cells were incubated with non-photoactivatable AC containing DNA (sequence 10, Table S1) while the CTO-labeled cells were incubated with GT DNA containing five photoprotected G groups (sequence 11, Table S1). Cells were incubated together in suspension and then exposed to 450 nm light for 60 s. After light exposure, cell aggregation was observed with a fluorescence microscope when dispensed onto a glass coverslip for imaging (Figures 4 and S5). In contrast, cells not exposed to light remained monodisperse when incubated together under identical conditions as the light exposed cells. This result demonstrates that cell−cell interactions are programmed by light exposure.

Based on our success of programming cell−cell interactions, we next sought to apply this technique in a spatially controlled fashion. We grew M4A4-GFP cells on Petri dishes until they reached high confluency. We then incubated the cells with MTET followed by GA DNA containing five photoprotected G groups (sequence 12, Table S1). Next, we exposed the cell

monolayer to 425 nm light with a DMD for 1 min. We then incubated the cell layer with CTO-labeled M4A4 cells that had been functionalized with complementary CT DNA (sequence 13, Table S1) for 5 min. After rinsing twice with PBS, we imaged the cells. Fluorescence micrographs revealed that CTO-labeled cells were localized to the areas exposed to light, demonstrating precise spatial control over cell behavior through DNA interactions (Figure 5). The attached cells were still localized to light-exposed areas after 1 h in media at 37 °C (Figure S6).

■ CONCLUSIONS

Our study demonstrates the successful use of oligonucleotides containing photocleavable protecting groups for spatiotemporally controlled hybridization in cell systems. By using guanines modified with coumarin protection groups, we were able to dynamically and spatially control the interaction between oligonucleotides with wavelengths that fall outside potentially cytotoxic UV regions. We also showed that the use of a DMD array allowed us to pattern oligonucleotides on glass substrates and selectively induce hybridization at desired locations using 365 and 425 nm lights. Overall, our study highlights the potential of using photocleavable protecting groups and patterning techniques to create highly controlled and precise hybridization events for bioengineering applications. Given the programmability of oligonucleotides, it is possible to combine different sequences along with multiple

rounds of cell additions to create more complex assemblies consisting of multiple different cell types spatially defined on surfaces. The ability to spatially and temporally control the interactions between oligonucleotides and cells offers a range of possibilities for creating complex biochips and cellular circuits for various biological studies.

■ METHODS

Safety

No unexpected, new, or significant hazards are associated with this work.

Cell Culture and Staining

NM2C5 cells (ATCC; CRL-2918) and M4A4-GFP cells (ATCC; CRL-2915) were maintained in Dulbecco's Modified Eagle's medium (DMEM) with 4.5 g/L glucose, L-glutamine, and sodium pyruvate (Corning), supplemented with 10% fetal bovine serum and 1% penicillin−streptomycin (PS). NIH-3T3 cells (ATCC; CRL-1658) were maintained in DMEM with 4.5 g/L glucose and L-glutamine without sodium pyruvate (Corning), supplemented with 1% Minimum Essential Medium nonessential amino acids (Corning), 10 μg/mL blasticidin, 10% FBS, and 1% PS. Cells were cultured at 37 °C and 5% CO2. Cells were passaged at 80% confluency, and media were changed every 2 to 3 days. Live cell staining was done with CellTracker (Invitrogen). CellTracker dye was resolubilized with dimethyl sulfoxide (DMSO) to a 10 mM stock concentration and diluted at 1:1000 with complete media. This working solution was added to the cells for 45 min at 37 °C. Cells were imaged using an Olympus BX63 microscope with the relevant filter sets. Cell imaging was completed on the same day for each experiment using the same microscope settings.

DNA Synthesis

All DNA monomers and reagents were purchased from Glen Research. DNA was synthesized with the Expedite synthesizer following manufacturer's standard protocols. We used standard bases along with the photoreactive coumarin-protected guanine (5′-dimethoxytrityl-N2-(4-isopropylphenoxyacetyl)-O6-[[7-(diethylamino)coumarin-4-yl]-methyl]-2′-deoxyGuanosine, 3'-[(2-cyanoethyl)-(N,N-diisopropyl)]-phosphoramidite). All oligonucleotides were synthesized with the dimethoxytrityl-on for purification. Oligonucleotides were deprotected using water saturated with ammonium hydroxide (28−32%; Fisher Chemicals) for 24 h at room temperature and then dried under air (Organomation). Oligonucleotides were then purified using a Glen-Pac DNA purification column (Glen Research) following the manufacturers protocols. Samples were subsequently lyophilized (Labconco, −105 °C) and reconstituted to target dilutions in water. For TCO-modified oligonucleotides, oligos were synthesized with a 5′ C6 amino-group (6-(4,4′-dimethoxy-4″-methylsulfonyl-tritylamino)hexyl-(2-cyanoethyl)-(N,N-diisopropyl)-phosphoramidite). After cleavage of the trityl group and purification, the oligonucleotides were incubated with TCO-PEG6-NHS ester with 10 μmol per 1 μmol of DNA synthesized in 10 mM HEPES-buffered saline (pH 8.4). Oligonucleotides were then purified on a GLEN Gel-Pak desalting column.

Surface Patterning of DNA

Glass coverslips were activated with plasma oxygen (Plasma Etch, Inc.) for 5 min. The coverslips were then incubated with 0.01% poly-l-lysine (Sigma-Aldrich) for 30 min, followed by incubation with 200 nM streptavidin (Invitrogen) for 30 min 10 μM biotinylated DNA with five photoprotected bases were incubated with streptavidin-coated slides. The surfaces were then exposed with either 365 nm (Sutter Instruments) or 450 nm LEDs (ThorLabs, laser power of 1445 mW) for different time intervals using a DMD (Mightex) attached to a microscope (BX63; Olympus). The cells were incubated with 1 μM Cy5-labeled complementary DNA for 2 min and then rinsed with 1× PBS (HyClone Cytiva). The PBS contains 144 mg/L potassium phosphate monobasic, 9000 mg/L sodium chloride, and 795 mg/L sodium phosphate dibasic. Stability of patterns was assessed by incubating at 37 °C overnight in complete growth media.

DNA Attachment to Cell Membranes

DNA is attached to the cell membrane through reactions involving methyltetrazine (MTET) sulfo-NHS ester. The NHS ester group reacts with primary amines of proteins on the cell surface and the MTET reacts with a TCO attached to the DNA, binding the DNA to the cell surface. A maximum of 600,000 cells were suspended in 100 μL of 1X PBS. A 200 mM stock solution of MTET-sulfo-NHS ester (Click Chemistry Tools) in anhydrous DMSO was added to the cells at 1 mM. After 10 min, the cells were rinsed twice by centrifuging at 250g for 5 min, removing the supernatant, and adding 100 μL of PBS. Incorporation of MTET was verified by incubating with TCO-Cy5 at 100 μM for 5 min, followed by flow cytometry (Guava EasyCyte). For DNA attachment assays, Cy5 TCO-DNA was added to the cells that were MTET functionalized (along with unfunctionalized controls) at 100 μM, left for 10 min, and rinsed twice with 1× PBS. Flow cytometry was performed to assess conjugation.

DNA Photoactivation Studies on Cell Surfaces

Cells were functionalized with DNA containing either 1, 3, or 5 photoprotected groups (as described above). For light-treated groups, the cells were then exposed to collimated 425 nm LED light (New Energy, laser power of 458 mW) for 1 min and then incubated with 1 μM complementary DNA labeled with Cy5 for 10 min. Following incubation, the cells were pelleted by centrifugation (500g for 5 min). The supernatant was removed, and the cells were rinsed with 1× PBS. This was repeated two times. Fluorescence intensity was assessed using flow cytometry.

For monolayer studies, NM2C5 cells grown into high confluency were functionalized with MTET by incubating with MTET-Sulfo-NHS for 10 min in 10 mM HEPES buffer (pH 8.4), with 150 mM NaCl. The cells were then triple rinsed with 1× PBS. Cells were functionalized with DNA containing five photoprotected groups and rinsed again with 1× PBS. The cells were then placed under a microscope (Olympus, BX63) equipped with a DMD (Mightex). Patterns were focused on the surface using 640 nm light (ThorLabs) to prevent unwanted deprotection. The surfaces were then exposed to patterns with 425 nm light with a 4× objective for 1, 5, 10, 30, and 60 s. The cells were then rinsed and then incubated with Cy5-labeled complementary DNA. The samples were rinsed with 1X PBS and imaged.

Cell Assembly

Cells were functionalized with DNA containing five protecting groups, as described above. The light treated group was exposed to 425 nm LED light for 1 min. Both light-treated and non-light-treated groups were incubated with cells functionalized with complementary DNA for 5 min. Then, the mixtures were pipetted onto a glass slide and covered with a coverslip for imaging with the Olympus BX63 microscope.

Cells on Monolayer

M4A4 cells were grown into high confluency and incubated with 1 mM MTET-Sulfo-NHS in 150 mM NaCl and 10 mM HEPES (pH 8.4) for 5 min at 30 °C. The cells were rinsed twice with 1X PBS and then incubated with 50 μM DNA containing five photoprotected groups. The cells were placed under a microscope with a DMD and exposed to 425 nm light with a 4× objective for 60 s. The cells were rinsed with 1× PBS and then incubated with cells functionalized with complementary DNA. After 5 min, the samples were rinsed with 1× PBS and imaged.

■ ASSOCIATED CONTENT

ⓢ Supporting Information

The Supporting Information is available free of charge at https://pubs.acs.org/doi/10.1021/acsmaterialsau.3c00020.

DNA sequences, micrographs of DNA printing, and flow cytometry density histograms (PDF)

■ AUTHOR INFORMATION

Corresponding Author

Brian Meckes − *Department of Biomedical Engineering, University of North Texas, Denton, Texas 76207, United States; BioDiscovery Institute, University of North Texas, Denton, Texas 76203, United States;* ⊕ orcid.org/0000-0002-8389-4622; Email: brian.meckes@unt.edu

Authors

Katelyn Mathis − *Department of Biomedical Engineering, University of North Texas, Denton, Texas 76207, United States; BioDiscovery Institute, University of North Texas, Denton, Texas 76203, United States*

Afia Ibnat Kohon − *Department of Biomedical Engineering, University of North Texas, Denton, Texas 76207, United States; BioDiscovery Institute, University of North Texas, Denton, Texas 76203, United States*

Stephen Black − *Department of Biomedical Engineering, University of North Texas, Denton, Texas 76207, United States; BioDiscovery Institute, University of North Texas, Denton, Texas 76203, United States*

Complete contact information is available at:
https://pubs.acs.org/10.1021/acsmaterialsau.3c00020

Author Contributions

§K.M. and A.I.K. have contributed equally. CRediT: **Katelyn Mathis** data curation (lead), formal analysis (lead), investigation (lead), methodology (equal), visualization (lead), writing-original draft (lead), writing-review & editing (equal); **Afia Ibnat Kohon** conceptualization (equal), data curation (lead), formal analysis (lead), investigation (lead), methodology (equal), writing-original draft (equal), writing-review & editing (equal); **Stephen Black** formal analysis (supporting), investigation (supporting), methodology (supporting), writing-review & editing (supporting); **Brian Meckes** conceptualization (lead), data curation (equal), formal analysis (equal), funding acquisition (lead), investigation (equal), methodology (lead), project administration (lead), resources (equal), software (equal), supervision (lead), visualization (equal), writing-original draft (equal), writing-review & editing (lead).

Author Contributions

The manuscript was written through contributions of all authors. All authors have given approval to the final version of the manuscript. CRediT: **Katelyn Mathis** data curation (lead), formal analysis (lead), investigation (lead), methodology (equal), visualization (lead), writing-original draft (lead), writing-review & editing (equal); **Afia Ibnat Kohon** conceptualization (equal), data curation (lead), formal analysis (lead), investigation (lead), methodology (equal), writing-original draft (equal), writing-review & editing (equal); **Stephen Black** formal analysis (supporting), investigation (supporting), methodology (supporting), writing-review & editing (supporting); **Brian Meckes** conceptualization (lead), data curation (equal), formal analysis (equal), funding acquisition (lead), investigation (equal), methodology (lead), project administration (lead), resources (equal), software (equal), supervision (lead), visualization (equal), writing-original draft (equal), writing-review & editing (lead).

Notes

The authors declare no competing financial interest.

■ REFERENCES

(1) Mitsiadis, T. A.; Muramatsu, T.; Muramatsu, H.; Thesleff, I. Midkine (MK), a Heparin-Binding Growth/Differentiation Factor, Is Regulated by Retinoic Acid and Epithelial-Mesenchymal Interactions in the Developing Mouse Tooth, and Affects Cell Proliferation and Morphogenesis. *J. Cell Biol.* **1995**, *129*, 267−281.

(2) Aoki, S.; Toda, S.; Sakemi, T.; Sugihara, H. Coculture of Endothelial Cells and Mature Adipocytes Actively Promotes Immature Preadipocyte Development In Vitro. *Cell Struct. Funct.* **2003**, *28*, 55−60.

(3) Jaiswal, A. S.; Marlow, B. P.; Gupta, N.; Narayan, S. β-Catenin-mediated transactivation and cell−cell adhesion pathways are important in curcumin (diferuylmethane)-induced growth arrest and apoptosis in colon cancer cells. *Oncogene* **2002**, *21*, 8414−8427.

(4) Sharkey, K. A.; Mawe, G. M. Neuroimmune and epithelial interactions in intestinal inflammation. *Curr. Opin. Pharmacol.* **2002**, *2*, 669−677.

(5) Hormuzdi, S. G.; Filippov, M. A.; Mitropoulou, G.; Monyer, H.; Bruzzone, R. Electrical synapses: a dynamic signaling system that shapes the activity of neuronal networks. *Biochim. Biophys. Acta, Biomembr.* **2004**, *1662*, 113−137.

(6) Braga, V. M.; Yap, A. S. The challenges of abundance: epithelial junctions and small GTPase signalling. *Curr. Opin. Cell Biol.* **2005**, *17*, 466−474.

(7) Klarlund, J. K.; Guilherme, A.; Holik, J. J.; Virbasius, J. V.; Chawla, A.; Czech, M. P. Signaling by Phosphoinositide-3,4,5-Trisphosphate Through Proteins Containing Pleckstrin and Sec7 Homology Domains. *Science* **1997**, *275*, 1927−1930.

(8) Stahl, A.; Wenger, A.; Weber, H.; Stark, G. B.; Augustin, H. G.; Finkenzeller, G. Bi-directional cell contact-dependent regulation of gene expression between endothelial cells and osteoblasts in a three-dimensional spheroidal coculture model. *Biochem. Biophys. Res. Commun.* **2004**, *322*, 684−692.

(9) Khodarev, N. N.; Yu, J.; Labay, E.; Darga, T.; Brown, C. K.; Mauceri, H. J.; Yassari, R.; Gupta, N.; Weichselbaum, R. R. Tumour-endothelium interactions in co-culture: coordinated changes of gene expression profiles and phenotypic properties of endothelial cells. *J. Cell Sci.* **2003**, *116*, 1013−1022.

(10) Chung, S.; Sudo, R.; Mack, P. J.; Wan, C.; Vickerman, V.; Kamm, R. D. Cell migration into scaffolds under co-culture conditions in a microfluidic platform. *Lab Chip* **2009**, *9*, 269−275.

(11) Zhang, K.; Chou, C.; Xia, X.; Hung, M.; Qin, L. Block-Cell-Printing for live single-cell printing. *Proc. Natl. Acad. Sci. U.S.A.* **2014**, *111*, 2948−2953.

(12) Sandig, M.; Voura, E. B.; Kalnins, V. I.; Siu, C. Role of cadherins in the transendothelial migration of melanoma cells in culture. *Cell Motil. Cytoskeleton* **1997**, *38*, 351−364.

(13) Berridge, M. V.; Herst, P. M.; Rowe, M. R.; Schneider, R.; McConnell, M. J. Mitochondrial transfer between cells: Methodological constraints in cell culture and animal models. *Anal. Biochem.* **2018**, *552*, 75−80.

(14) Yang, H.; Borg, T. K.; Ma, Z.; Xu, M.; Wetzel, G.; Saraf, L. V.; Markwald, R.; Runyan, R. B.; Gao, B. Z. Biochip-based study of unidirectional mitochondrial transfer from stem cells to myocytes via tunneling nanotubes. *Biofabrication* **2016**, *8*, 015012.

(15) Jing, D.; Fonseca, A.; Alakel, N.; Fierro, F. A.; Muller, K.; Bornhauser, M.; Ehninger, G.; Corbeil, D.; Ordemann, R. Hematopoietic stem cells in co-culture with mesenchymal stromal

cells - modeling the niche compartments in vitro. *Haematologica* **2010**, *95*, 542−550.

(16) Kirkpatrick, C. J.; Fuchs, S.; Unger, R. E. Co-culture systems for vascularization—Learning from nature. *Adv. Drug Delivery Rev.* **2011**, *63*, 291−299.

(17) Borciani, G.; Montalbano, G.; Baldini, N.; Cerqueni, G.; Vitale-Brovarone, C.; Ciapetti, G. Co−culture systems of osteoblasts and osteoclasts: Simulating in vitro bone remodeling in regenerative approaches. *Acta Biomater.* **2020**, *108*, 22−45.

(18) Hsiao, A. Y.; Torisawa, Y.; Tung, Y.; Sud, S.; Taichman, R. S.; Pienta, K. J.; Takayama, S. Microfluidic system for formation of PC-3 prostate cancer co-culture spheroids. *Biomaterials* **2009**, *30*, 3020−3027.

(19) Tirziu, D.; Giordano, F. J.; Simons, M. Cell communications in the heart. *Circulation* **2010**, *122*, 928−937.

(20) Plotnikov, E. Y.; Khryapenkova, T. G.; Vasileva, A. K.; Marey, M. V.; Galkina, S. I.; Isaev, N. K.; Sheval, E. V.; Polyakov, V. Y.; Sukhikh, G. T.; Zorov, D. B. Cell-to-cell cross-talk between mesenchymal stem cells and cardiomyocytes in co-culture. *J. Cell. Mol. Med.* **2008**, *12*, 1622−1631.

(21) Wynn, T. A. Integrating Mechanisms of Pulmonary Fibrosis. *J. Exp. Med.* **2011**, *208*, 1339−1350.

(22) Simpson, E. Special regulatory T-cell review: regulation of immune responses − examining the role of T cells. *Immunology* **2008**, *123*, 13−16.

(23) Fouchet, D.; Regoes, R. A Population Dynamics Analysis of the Interaction between Adaptive Regulatory T Cells and Antigen Presenting Cells. *PLoS One* **2008**, *3*, No. e2306.

(24) Mayer, J. U.; Demiri, M.; Agace, W. W.; MacDonald, A. S.; Svensson-Frej, M.; Milling, S. W. Different populations of CD11b+ dendritic cells drive Th2 responses in the small intestine and colon. *Nat. Commun.* **2017**, *8*, 15820.

(25) Lane, S. W.; Williams, D. A.; Watt, F. M. Modulating the stem cell niche for tissue regeneration. *Nat. Biotechnol.* **2014**, *32*, 795−803.

(26) Kim, M.; Bae, Y. K.; Um, S.; Kwon, J. H.; Kim, G.; Choi, S. J.; Oh, W.; Jin, H. J. A Small-Sized Population of Human Umbilical Cord Blood-Derived Mesenchymal Stem Cells Shows High Stemness Properties and Therapeutic Benefit. *Stem Cells Int.* **2020**, *2020*, 1−17.

(27) Hui, E. E.; Bhatia, S. N. Micromechanical control of cell-cell interactions. *Proc. Natl. Acad. Sci. U.S.A.* **2007**, *104*, 5722−5726.

(28) Rao, N.; Grover, G. N.; Vincent, L. G.; Evans, S. C.; Choi, Y. S.; Spencer, K. H.; Hui, E. E.; Engler, A. J.; Christman, K. L. A co-culture device with a tunable stiffness to understand combinatorial cell−cell and cell−matrix interactions. *Integr. Biol.* **2013**, *5*, 1344−1354.

(29) Ahn, G.; Min, K.; Kim, C.; Lee, J.; Kang, D.; Won, J.; Cho, D.; Kim, J.; Jin, S.; Yun, W.; Shim, J. Precise stacking of decellularized extracellular matrix based 3D cell-laden constructs by a 3D cell printing system equipped with heating modules. *Sci. Rep.* **2017**, *7*, 8624−8711.

(30) Kim, B. S.; Kwon, Y. W.; Kong, J.; Park, G. T.; Gao, G.; Han, W.; Kim, M.; Lee, H.; Kim, J. H.; Cho, D. 3D cell printing of in vitro stabilized skin model and in vivo pre-vascularized skin patch using tissue-specific extracellular matrix bioink: A step towards advanced skin tissue engineering. *Biomaterials* **2018**, *168*, 38−53.

(31) Chandra, R. A.; Douglas, E. S.; Mathies, R. A.; Bertozzi, C. R.; Francis, M. B. Programmable Cell Adhesion Encoded by DNA Hybridization. *Angew. Chem., Int. Ed.* **2006**, *45*, 896−901.

(32) Gartner, Z. J.; Bertozzi, C. R. Programmed assembly of 3-dimensional microtissues with defined cellular connectivity. *Proc. Natl. Acad. Sci. U.S.A.* **2009**, *106*, 4606−4610.

(33) Qiao, C.; Wu, J.; Huang, Z.; Cao, X.; Liu, J.; Xiong, B.; He, Y.; Yeung, E. S. Sequence-Modulated Interactions between Single Multivalent DNA-Conjugated Gold Nanoparticles. *Anal. Chem.* **2017**, *89*, 5592−5597.

(34) Todhunter, M. E.; Jee, N. Y.; Hughes, A. J.; Coyle, M. C.; Cerchiari, A.; Farlow, J.; Garbe, J. C.; LaBarge, M. A.; Desai, T. A.; Gartner, Z. J. Programmed synthesis of three-dimensional tissues. *Nat. Methods* **2015**, *12*, 975−981.

(35) Prahl, L. S.; Porter, C. M.; Liu, J.; Viola, J. M.; Hughes, A. J. Independent control over cell patterning and adhesion on hydrogel substrates for tissue interface mechanobiology. *iScience* **2023**, *26*, 106657−106723.

(36) Kozminsky, M.; Scheideler, O. J.; Li, B.; Liu, N. K.; Sohn, L. L. Multiplexed DNA-Directed Patterning of Antibodies for Applications in Cell Subpopulation Analysis. *ACS Appl. Mater. Interfaces* **2021**, *13*, 46421−46430.

(37) Scheideler, O. J.; Yang, C.; Kozminsky, M.; Mosher, K. I.; Falcón-Banchs, R.; Ciminelli, E. C.; Bremer, A. W.; Chern, S. A.; Schaffer, D. V.; Sohn, L. L. Recapitulating complex biological signaling environments using a multiplexed, DNA-patterning approach. *Sci. Adv.* **2020**, *6*, No. eaay5696.

(38) Song, P.; Shen, J.; Ye, D.; Dong, B.; Wang, F.; Pei, H.; Wang, J.; Shi, J.; Wang, L.; Xue, W.; Huang, Y.; Huang, G.; Zuo, X.; Fan, C. Programming bulk enzyme heterojunctions for biosensor development with tetrahedral DNA framework. *Nat. Commun.* **2020**, *11*, 838.

(39) Tang, X.; Richards, J. L.; Peritz, A. E.; Dmochowski, I. J. Photoregulation of DNA polymerase I (Klenow) with caged fluorescent oligodeoxynucleotides. *Bioorg. Med. Chem. Lett.* **2005**, *15*, 5303−5306.

(40) Lusic, H.; Young, D. D.; Lively, M. O.; Deiters, A. Photochemical DNA Activation. *Org. Lett.* **2007**, *9*, 1903−1906.

(41) Kröck, L.; Heckel, A. Photoinduced Transcription by Using Temporarily Mismatched Caged Oligonucleotides. *Angew. Chem., Int. Ed.* **2005**, *44*, 471−473.

(42) Fichte, M. A. H.; Weyel, X. M. M.; Junek, S.; Schäfer, F.; Herbivo, C.; Goeldner, M.; Specht, A.; Wachtveitl, J.; Heckel, A. Three-Dimensional Control of DNA Hybridization by Orthogonal Two-Color Two-Photon Uncaging. *Angew. Chem., Int. Ed.* **2016**, *55*, 8948−8952.

(43) Rodrigues-Correia, A.; Weyel, X. M. M.; Heckel, A. Four Levels of Wavelength-Selective Uncaging for Oligonucleotides. *Org. Lett.* **2013**, *15*, 5500−5503.

(44) Menge, C.; Heckel, A. Coumarin-Caged dG for Improved Wavelength-Selective Uncaging of DNA. *Org. Lett.* **2011**, *13*, 4620−4623.

(45) Keyhani, S.; Goldau, T.; Blümler, A.; Heckel, A.; Schwalbe, H. Chemo-Enzymatic Synthesis of Position-Specifically Modified RNA for Biophysical Studies including Light Control and NMR Spectroscopy. *Angew. Chem., Int. Ed.* **2018**, *57*, 12017−12021.

(46) Schäfer, F.; Wagner, J.; Knau, A.; Dimmeler, S.; Heckel, A. Regulating Angiogenesis with Light-Inducible AntimiRs. *Angew. Chem., Int. Ed.* **2013**, *52*, 13558−13561.

(47) Johann, K.; Svatunek, D.; Seidl, C.; Rizzelli, S.; Bauer, T. A.; Braun, L.; Koynov, K.; Mikula, H.; Barz, M. Tetrazine- and trans-cyclooctene-functionalised polypept(o)ides for fast bioorthogonal tetrazine ligation. *Polym. Chem.* **2020**, *11*, 4396−4407.